Focusing of a neutral helium beam with a photon-sieve structure

Article *in* Physical Review A · April 2015

DOI: 10.1103/PhysRevA.91.043608

7 authors, including:

Sabrina Eder
University of Bergen
21 PUBLICATIONS **263** CITATIONS
SEE PROFILE

X.D. Guo
University of Bergen
22 PUBLICATIONS **151** CITATIONS
SEE PROFILE

Thomas Kaltenbacher
CERN
32 PUBLICATIONS **136** CITATIONS
SEE PROFILE

Martin M. Greve
University of Bergen
12 PUBLICATIONS **62** CITATIONS
SEE PROFILE

Focusing of a neutral helium beam with a photon-sieve structure

S. D. Eder,[1] X. Guo,[1] T. Kaltenbacher,[1,*] M. M. Greve,[1] M. Kalläne,[2,3] L. Kipp,[2,3] and B. Holst[1,†]
[1]*Department of Physics and Technology, University of Bergen, Allégaten 55, 5007 Bergen, Norway*
[2]*Institute for Experimental and Applied Physics, University of Kiel, Leibnizstrasse 19, 24098 Kiel, Germany*
[3]*Ruprecht Haensel Laboratory, University of Kiel and DESY, Kiel, Germany*
(Received 27 January 2015; published 8 April 2015)

The manipulation of low-energy beams of neutral atoms and molecules via their de Broglie wavelength is a branch of atom optics often referred to as de Broglie matter wave optics. The application areas include fundamental quantum mechanics, atom interferometry, and the development of new microscopy instrumentation. The focusing of de Broglie matter waves with a Fresnel zone plate was used to demonstrate the first neutral helium microscopy imaging. The ultimate resolution of such a microscope is limited by the width of the outermost zone. Because a Fresnel zone plate for atoms cannot be fabricated on a substrate (the low-energy atom beams would not be able to penetrate the substrate material), this gives a fabrication determined limit for the first-order focus of around 30–50 nm. Therefore, it is important to search for alternative optical elements that enable higher resolution. Photon sieves consist of a large number of pinholes, arranged suitably relative to the Fresnel zones. The great advantages are that the width of the pinholes can be larger than the respective Fresnel zones and a free-standing pinhole is much easier to fabricate than a free-standing zone. Thus, with a photon-sieve structure applied for de Broglie matter wave manipulation, the fabrication limit for focusing is reduced to potentially around 3–5 nm. Here we present a realization of such an "atom sieve," which we fabricated out of a silicon nitride (SiN) membrane, using electron-beam lithography and reactive ion etching. Our atom sieve is 178 μm in diameter and has 31 991 holes. The diameter of the holes varies from 1840 to 150 nm. Using a beam of neutral, ground-state helium atoms with an average wavelength of 0.055 nm, we demonstrate helium atom focusing down to a spot size of less than 4 μm. The focus size is limited by the intrinsic velocity spread of the helium beam.

DOI: 10.1103/PhysRevA.91.043608 PACS number(s): 03.75.Be, 07.77.Gx

I. INTRODUCTION

The use of nanostructured optical elements for the manipulation of low-energy beams of neutral atoms and molecules, exploiting their de Broglie wavelength, has increased extensively over the last two decades. For a recent review of de Broglie matter wave optics, see [1]. Particularly famous experiments include the proof of the existence of the helium dimer and the diffraction of C_{60} molecules [2,3]. Both of these experiments used nanostructured transmission gratings. In 2008, the first neutral helium microscopy images were obtained using a Fresnel zone plate to focus a helium beam down to a few μm [4] and later even below one μm [5]. The beam was created by free-jet (also referred to as supersonic) expansion from a helium gas reservoir kept at a constant temperature and pressure. The wavelength of the helium beam created in such expansions is typically less than 0.1 nm and the energy is less than 100 meV. This makes neutral helium microscopy potentially a very attractive method for the investigation of fragile, insulating substrates and high aspect ratio structures. See [6,7] for overviews of the application of neutral helium beams in surface science studies. Fresnel zone plates have also been used to map the free-jet (supersonic) expansion of molecular beams [8,9] and it has been suggested that the Poisson spot phenomenon (a configuration where a circular plate blocks the central area around the optical axis for a point source) can be used to test the quantum mechanical properties of large molecules [10]. The first experimental realization of the Poisson spot for matter waves was done in 2009 using a deuterium beam [11].

Alternatively to Fresnel zone plates, mirrors can be used as focusing elements [12–14]. The advantage of mirrors is that in contrast to Fresnel zone plate based optical elements, they have no chromatic aberration so that the velocity spread of the beam does not play a role, though there will be a certain signal loss through diffraction and scattering from steps and point defects as well as inelastic scattering. The use of graphene as a mirror coating gives an inert and very stable surface [15]. Particularly attractive is the use of quantum reflection for focusing [16]. Quantum reflection can, in principle, be completely loss free.

Unfortunately, up until now, it has not been possible to control the curvature of mirrors with high enough precision, so that Fresnel zone plate based optical elements remain the most promising approach for the focusing of neutral atom and molecular beams. Because of the low energy of the beams (typically less than 100 meV per particle), it cannot penetrate through any solid material and therefore the optical element, for example a Fresnel zone plate, has to be a free-standing, suspended structure and cannot be placed on a substrate. This is a particular fabrication challenge, which limits the width of the outermost zone and means that the Fresnel zone plates can only be constructed with additional support rods. It also means that the only Fresnel zone plates that can be applied are so-called binary-type zone plates (either an area is opaque or completely open). The simplest binary-type Fresnel zone plate based optical element is the standard Fresnel zone plate (Fresnel-Soret zone plate), which is also the only one that has been applied in de Broglie matter wave optics before this work, though there exist other promising candidates [17,18].

*thomas.kaltenbacher@uib.no
†bodil.holst@uib.no

The photon sieve was invented in 2001, originally intended for applications with soft x-rays [19]. It is a structure consisting of pinholes of varying size arranged across the Fresnel zones in such a manner that it is possible to focus to a spot with a diameter smaller than the smallest pinhole. In addition, higher-order diffraction and secondary maxima can be suppressed by several orders of magnitude. The original photon sieve is based on a standard Fresnel zone plate; since then, other configurations have been suggested, for example, a Beynon-Gabor zone plate based photon sieve [20] or a reflective photon sieve [21].

In this paper, we demonstrate an application of the photon-sieve structure as an atom sieve. Our structure is based on a standard Fresnel zone plate similar to the first photon sieve presented in [19] using a Weber-type transmission window. In Sec. II, we present the molecular beam apparatus, where the focusing experiments were carried out. Section III contains a short description of how the atom sieve was made. The theoretical background is briefly explained in Sec. IV. In Sec. V, the atom-sieve focusing results are presented. The paper finishes with a conclusion (Sec. VI) and acknowledgments.

II. EXPERIMENTAL SETUP

The experiments presented here were carried out in the molecular beam apparatus MAGIE. A diagram of the setup can be seen in Fig. 1; for a detailed description of the instrument, see [22]. The neutral helium beam was created by a free-jet (also referred to as supersonic) expansion from a source reservoir at 81 ± 1 bar through a 10-μm-diameter nozzle. The central part of the beam was selected by a skimmer, 4 ± 0.5 μm in diameter, placed 11.5 ± 0.5 mm in front of the nozzle. A collimating aperture, 400 ± 5 μm in diameter, was placed 962 ± 2 mm down the beam line. All experiments were carried out at room temperature corresponding to an average He beam energy of ≈66.9 meV corresponding to a wavelength of $\lambda \approx 0.0553 \pm 0.0004$ nm and a velocity of 1796 ± 6 m/s. The velocity spread of the beam was $\Delta v \approx 50$ m/s corresponding to a wavelength spread of $\Delta\lambda \approx 0.0015$ nm. The velocity and velocity spread of the beam were determined independently by time-of-flight (TOF) measurements.

Our atom sieve is designed to have a focal length of about 482 mm for $\lambda = 0.0553$ nm. For an object distance g (the distance between the skimmer and the atom sieve) of 1532 mm, this corresponds to an image distance b (the distance between atom sieve and detector) of about 703 mm. A Weber-type transmission window was used [19].

The measurements were carried out by scanning a 10 ± 1-μm-wide slit aperture mounted on a piezo table across the focused spot in 500 nm steps, measuring 5 seconds per step. The distance between the skimmer and the atom sieve was kept fixed at 1532 ± 5 mm. The distance between the atom sieve and the detector can be varied manually. The measurements presented here were all taken close to the theoretically expected image distance. Variations of 10 mm in both directions did not change the spot size, which is not surprising given the velocity spread of the beam and the very small numerical aperture of the atom sieve, leading to a large depth of field.

III. ATOM-SIEVE FABRICATION

A free-standing silicon nitride membrane, about 200 nm thick, was prepared by a standard microprocessing etch step using potassium hydroxide (KOH) to etch silicon from a silicon wafer, for freeing the silicon nitride layer. A 20-nm-thick chrome layer was evaporated on top of the silicon nitride using an electron-beam evaporator (Temescal FC2000). Then a 150-nm-thick layer of polymethylmethacrylate (PMMA) was spin coated on top of the chrome layer and the atom-sieve pattern was written in the PMMA using electron-beam (*e*-beam) lithography (Raith *e*-line). The pattern was loaded as a cif file (similar to a txt file). The cif file contains the center coordinates and size of each hole. The design parameters can be found in Table I. The pattern was calculated on the basis of these design parameters using the procedure described in [19,21]. The exposure dose for the *e*-beam writing was 100 μC/cm^2 with a beam voltage of 10 kV. Determining

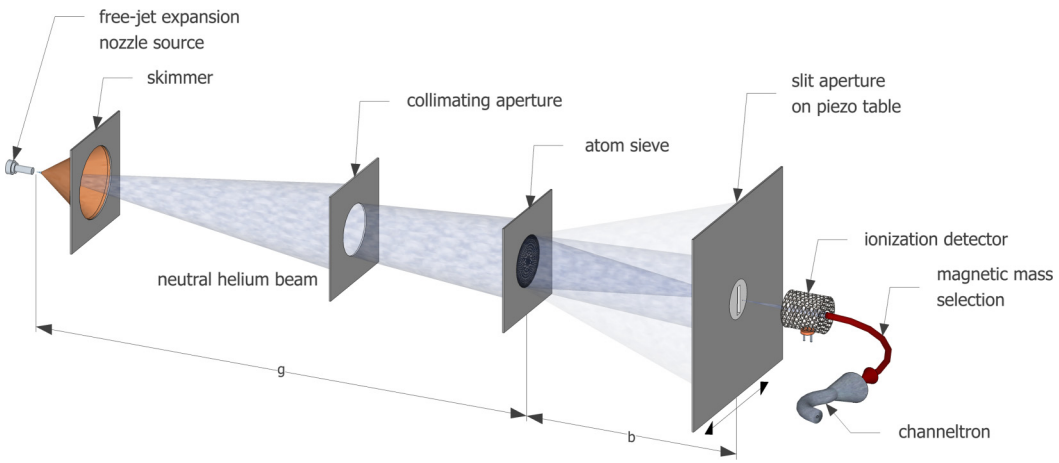

FIG. 1. (Color online) Diagram of the experimental setup (not to scale). After the free-jet expansion through the nozzle, the central part of the helium beam is selected by the skimmer. Behind the skimmer, the beam is collimated using a 400-μm-diameter aperture. The focused helium atom spot is observed by moving a 10 μm slit aperture mounted on a piezo table across the image plane in 500 nm steps. After the slit aperture, the helium atoms are ionized, mass selected, and, finally, detected in a channeltron.

TABLE I. Atom-sieve parameters.

Parameter	Value
First-order focal length for $\lambda = 0.0553$ nm	482 mm
Overall diameter, D_{sieve}	178 μm
Theoretical total transmission	9.22%
Central stop diameter	13 μm
Number of pinholes	31991
Smallest pinhole diameter	150 ± 5 nm
Largest pinhole diameter	1840 ± 5 nm

the optimum exposure dose so that the correct hole size is obtained is critical and strongly dependent on factors such as substrate material, acceleration voltage, resist thickness, etc. Following the *e*-beam exposure, the sample was developed for 60 s using an AR 600-56 developer. Afterwards, the sample was put in chrome etchant for 25 s at room temperature. This removed the chrome from the membrane in the areas where the PMMA had been removed in the preceding development step. The remaining chrome under the PMMA acted as a protective layer in the final step, where the holes were created by etching the silicon nitride material in the exposed areas as well as the residual PMMA using reactive-ion etching (Plasmatherm 790+). A subsequent chemical chrome etch step was used to remove the remaining chrome from the silicon nitride membrane. The reactive-ion etching was carried out using high-purity CF_4 gas at 100 W, 15 standard cubic centimeters per minute (SCCM) at 10 mtorr base pressure. The etching time was 18 min. The thickness of the chrome layer needs to be adjusted so that it is thick enough to act as a protective layer during the entire etching process. An alternative way to create hole patterns in silicon nitride membranes is described in [23]. An image of the atom sieve can be seen in Fig. 2.

IV. THEORETICAL BACKGROUND

The size of the focused helium atom spot is determined by the geometry of the system, the size of the imaged object, and the chromatic aberration caused by the velocity spread of the beam.

The speed ratio S of the helium beam is a measure for the monochromaticity of the beam. S is defined as $S = 2\sqrt{\ln(2)}\, v/\Delta v$ [24], where Δv is the full width at half maximum (FWHM) of the measured velocity distribution and v is the average beam velocity. The chromatic aberration for a photon sieve is the same as for a Fresnel zone plate [19]. Hence, it can be described by the transversal width of the chromatic point spread function (PSF). Following [25], we get

$$d_{p,\text{sieve}} = \sqrt{\ln(2)}\frac{D_{\text{sieve}}}{S}, \tag{1}$$

where $d_{p,\text{sieve}}$ is the transversal width of the chromatic point spread function and D_{sieve} is the overall diameter of the sieve. The final focused spot size, $d_{\text{th,tot}}$, will be a convolution of PSF with the imaged object. A simplified model for the final focused spot size is given by approximating the object and PSF with Gaussian functions. The skimmer diameter, d_{sk}, is taken to be the FWHM of the object function [5].

We thus obtain, for the theoretical, final spot size,

$$d_{\text{th,tot}} = \sqrt{d_{p,\text{sieve}}^2 + (M d_{\text{sk}})^2}, \tag{2}$$

where $M = b/g$ denotes the magnification of the experimental configuration (Fig. 1).

For the measurement presented here, we have $S = 60 \pm 4$ (obtained using time-of-flight measurements). $M = 0.460 \pm 0.004$, $D_{\text{sieve}} = 178$ μm, and $d_{\text{sk}} = 4 \pm 0.5$ μm, giving a theoretically predicted focal spot size, $d_{\text{th,tot}} = 3.1 \pm 0.5$ μm.

V. RESULTS AND ANALYSIS

Figure 3 shows the experimental result obtained by scanning a 10-μm-wide slit across the focused spot as described in Sec. II. The graph represents the average of 47 scans. The intensity of the signal is quite low because only about 1% of the incident beam gets into the focus.

The focused spot size is obtained from the experimental data as follows: The resulting intensity distribution $I(x)$ obtained in Fig. 3 is a result of the convolution of the slit transmission function with the Gaussian intensity distribution of the focus. Since the slit width w is larger than the total focal spot size in

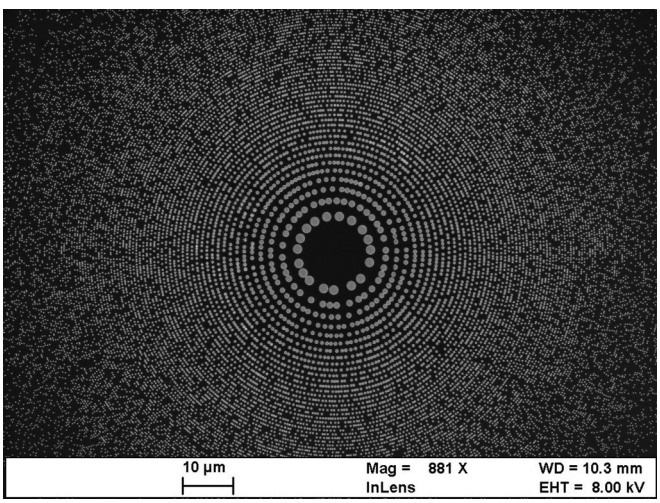

FIG. 2. Scanning electron microscopy image of the atom sieve used in this experiment as seen before the chrome etching.

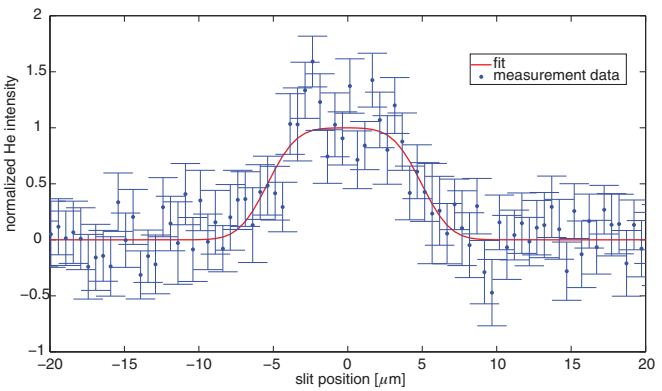

FIG. 3. (Color online) Experimental data with fit corresponding to a focused spot size of 3.6 μm.

our experiment, the resulting intensity profile of the horizontal scan as a function of the slit position x is given by

$$I(x) = \frac{1}{2}\left[\mathrm{erf}\left(\frac{x+\frac{w}{2}}{\sqrt{2}\sigma}\right) - \mathrm{erf}\left(\frac{x-\frac{w}{2}}{\sqrt{2}\sigma}\right)\right], \qquad (3)$$

where $\mathrm{erf}(x) = 2/\sqrt{\pi}\int_0^x \exp(-t^2)dt$ denotes the (Gaussian) error function, and σ is the Gaussian standard deviation.

The function $I(x)$ is used to fit the measured intensity profile (red solid line) shown in Fig. 3 to obtain the parameter σ, which is a measure for the slope, bearing the information about the FWHM of the focal spot; see [4]. The total focal spot size, d_{tot}, is then calculated as

$$d_{\mathrm{tot}} = 2\sqrt{2\ln(2)}\sigma\ . \qquad (4)$$

The best fit is presented in Fig. 3 and corresponds to a measured spot size of 3.6 ± 0.8 μm, in good agreement with the theoretically predicted spot size of 3.1 ± 0.5 μm.

VI. CONCLUSION

We present an experimental realization of an optical element for de Broglie matter wave manipulation: the atom sieve. We demonstrate focusing down to less than 4 μm, in good agreement with our theoretical predictions. For the experiment presented here, the velocity spread of the helium beam was the limiting factor for the focused spot size. A higher speed ratio (monochromaticity) of the helium beam can be obtained in various ways [26–28] so that better focusing should be possible in the future. For the highest resolutions, velocity selection of the beam will be necessary, which will reduce the focused beam intensity. However, our calculations show that by using a rectangular transmission window instead of a Weber-type transmission window, the overall transmission of an atom sieve can be increased from 9% to 27%, which is only about a factor of two less than a standard Fresnel-Soret zone plate. The increase in intensity when changing the transmission window is discussed in [19]. The price to pay is that the higher-order maxima are no longer suppressed, but this is not a major issue for microscopy applications. It should also be noted that it will be possible to fabricate the atom sieve with a larger overall area than the Fresnel-Soret zone plate, as discussed in the Abstract. As the holes in the atom sieve gets smaller the van der Waal interaction will start to play a role, leading to a shrinking of the effective hole size. This can be compensated for by making the holes slightly larger. The interaction potential between Helium and Silicon Nitride is well known [29]. Thus we conclude that the way is open for the use of atom sieves in helium microscopy and thereby for helium microscopy with 3–5 nm resolution.

ACKNOWLEDGMENTS

The work presented here was sponsored by the European Union: Theme NMP.2012.1.4-3, Grant No. 309672, project NEMI (Neutral Microscopy). The atom sieve was fabricated using the UiB Nanostructures Laboratory. We acknowledge support from the Bergen Research Foundation with Trond Mohn and the Research Council of Norway. X.G. was funded by The Research Council of Norway (The Michelsen Center).

S.D.E., X.G., and T.K. contributed equally to this work.

[1] A. D. Cronin, J. Schmiedmayer, and D. E. Pritchard, Rev. Mod. Phys. **81**, 1051 (2009).
[2] W. Schöllkopf and J. P. Toennies, Science **266**, 1345 (1994).
[3] M. Arndt, O. Nairz, J. Vos-Andreae, C. Keller, G. van der Zouw, and A. Zeilinger, Nature (London) **401**, 680 (1999).
[4] M. Koch, S. Rehbein, G. Schmahl, T. Reisinger, G. Bracco, W. E. Ernst, and B. Holst, J. Microsc. **229**, 1 (2008).
[5] S. D. Eder, T. Reisinger, M. M. Greve, G. Bracco, and B. Holst, New J. Phys. **14**, 073014 (2012).
[6] D. Farias and K.-H. Rieder, Rep. Prog. Phys. **61**, 1575 (1998).
[7] B. Holst and G. Bracco, in *Surface Science Techniques*, Springer Series in Surface Sciences, Vol. 51, edited by G. Bracco and B. Holst (Springer, Berlin, Heidelberg, 2013), pp. 333–365.
[8] T. Reisinger, G. Bracco, S. Rehbein, G. Schmahl, W. E. Ernst, and B. Holst, J. Phys. Chem. A **111**, 12620 (2007).
[9] S. D. Eder, G. Bracco, T. Kaltenbacher, and B. Holst, J. Phys. Chem. A **118**, 4 (2014).
[10] T. Reisinger, G. Bracco, and B. Holst, New J. Phys. **13**, 065016 (2011).
[11] T. Reisinger, A. A. Patel, H. Reingruber, K. Fladischer, W. E. Ernst, G. Bracco, H. I. Smith, and B. Holst, Phys. Rev. A **79**, 053823 (2009).
[12] R. B. Doak, in *Helium Atom Scattering from Surfaces*, Springer Series in Surface Sciences, Vol. 27, edited by E. Hulpke (Springer, Berlin, Heidelberg, 1992).
[13] B. Holst and W. Allison, Nature (London) **390**, 244 (1997).
[14] K. Fladischer, H. Reingruber, T. Reisinger, V. Mayrhofer, W. E. Ernst, A. E. Ross, D. A. MacLaren, W. Allison, D. Litwin, J. Galas, S. Sitarek, P. Nieto, D. Barredo, D. Farías, R. Miranda, B. Surma, A. Miros, B. Piatkowski, E. Søndergård, and B. Holst, New J. Phys. **12**, 033018 (2010).
[15] P. Sutter, M. Minniti, P. Albrecht, D. Faras, R. Miranda, and E. Sutter, Appl. Phys. Lett. **99**, 211907 (2011).
[16] H. C. Schewe, B. S. Zhao, G. Meijer, and W. Schöllkopf, New J. Phys. **11**, 113030 (2009).
[17] M. M. Greve, A. M. Vial, J. J. Stamnes, and B. Holst, Opt. Express **21**, 28483 (2013).
[18] X. Chen and X. Wang, Opt. Express **21**, 20005 (2013).
[19] L. Kipp, M. Skibowski, R. L. Johnson, R. Berndt, R. Adelung, S. Harm, and R. Seemann, Nature (London) **414**, 184 (2001).
[20] W. Fan, L. Wei, H. Zang, L. Cao, B. Zhu, X. Zhu, C. Xie, Y. Gao, Z. Zhao, and Y. Gu, Opt. Express **21**, 1473 (2013).
[21] M. Kalläne, J. Buck, S. Harm, R. Seemann, K. Rossnagel, and L. Kipp, Opt. Lett. **36**, 2405 (2011).
[22] A. Apfolter, M.S. thesis, Graz University of Technology, 2005.
[23] J. Olav Grepstad, M. M. Greve, T. Reisinger, and B. Holst, J. Vac. Sci. Technol. B **31**, 06F402 (2013).
[24] H. Pauly, in *Atom, Molecule, and Cluster Beams I*, Springer Series on Atomic, Optical, and Plasma Physics, edited by

G. F. Drake and G. Ecker, Vol. 28 (Springer, Berlin, Heidelberg, 2000).

[25] A. Michette, *Optical Systems for Soft X Rays* (Plenum, New York, 1986).

[26] T. Reisinger and B. Holst, J. Vac. Sci. Technol. B **26**, 2374 (2008).

[27] V. L. Hirschy and J. P. Aldridge, Rev. Sci. Instrum. **42**, 381 (1971).

[28] G. Rotzoll, J. Phys. E: Sci. Instrum. **15**, 708 (1982).

[29] R. E. Grisenti, W. Schöllkopf, J. P. Toennies, G. C. Hegerfeldt, and T. Köhler, Phys. Rev. Lett. **83**, 1755 (1999).